XMeis3 protein activity is required for proper hindbrain patterning in *Xenopus laevis* embryos

Charna Dibner, Sarah Elias and Dale Frank*

Department of Biochemistry, Rappaport Faculty of Medicine, Technion-Israel Institute of Technology, Haifa 31096, Israel
*Author for correspondence (e-mail: dale@tx.technion.ac.il)

SUMMARY

Meis-family homeobox proteins have been shown to regulate cell fate specification in vertebrate and invertebrate embryos. Ectopic expression of RNA encoding the *Xenopus* Meis3 (XMeis3) protein caused anterior neural truncations with a concomitant expansion of hindbrain and spinal cord markers in *Xenopus* embryos. In naïve animal cap explants, *XMeis3* activated expression of posterior neural markers in the absence of pan-neural markers. Supporting its role as a neural caudalizer, *XMeis3* is expressed in the hindbrain and spinal cord. We show that XMeis3 acts like a transcriptional activator, and its caudalizing effects can be mimicked by injecting RNA encoding a VP16-XMeis3 fusion protein. To address the role of endogenous XMeis3 protein in neural patterning, XMeis3 activity was antagonized by injecting RNA encoding an Engrailed-XMeis3 antimorph fusion protein or *XMeis3* antisense morpholino oligonucleotides. In these embryos, anterior neural structures were expanded and posterior neural tissues from the midbrain-hindbrain junction through the hindbrain were perturbed. In neuralized animal cap explants, XMeis3-antimorph protein modified caudalization by basic fibroblast growth factor and Wnt3a. XMeis3-antimorph protein did not inhibit caudalization per se, but re-directed posterior neural marker expression to more anterior levels; it reduced expression of spinal cord and hindbrain markers, yet increased expression of the more rostral *En2* marker. These results provide evidence that XMeis3 protein in the hindbrain is required to modify anterior neural-inducing activity, thus, enabling the transformation of these cells to posterior fates.

Key words: *Xenopus laevis*, XMeis3, Antimorph, Antisense morpholino oligonucleotides, Caudalization, Hindbrain

INTRODUCTION

Formation of the central nervous system (CNS) in vertebrates such as *Xenopus* is initiated during gastrulation and largely depends on the inductive interaction between the ectoderm and adjacent dorsal mesoderm (Spemann organizer). The CNS is characterized by distinct anteroposterior (AP) and dorsoventral patterning (review by Hamburger, 1988; Doniach, 1993). The predominant concept of how AP patterning is established was suggested by Nieuwkoop (Nieuwkoop, 1952). In this two-step model, the initial neural inducing signal is thought to specify anterior neuroectodermal structures, such as cement gland and forebrain; this first step is referred to as 'activation'. The second caudalizing step is called 'transformation.' During this second step, anterior neural tissue is respecified to more posterior fates, such as midbrain, hindbrain and spinal cord.

Several molecules have been identified which participate in the 'activation' and 'transformation' processes. Non-neural ectoderm is induced to anterior-neural tissue by inhibition of bone morphogenetic protein (BMP) activity (reviewed by Harland and Gerhart, 1997). Secreted BMP antagonist molecules bind the BMP molecule and inhibit its receptor binding activity (Zimmerman et al., 1996; Piccolo et al., 1996; Fainsod et al., 1997; Hsu et al., 1998). BMP antagonists are

expressed in Spemann's organizer during gastrulation and induce anterior neural tissue in adjacent ectoderm (Lamb et al., 1994; Hemmati-Brivanlou and Melton, 1994; Sasai et al., 1994).

Three secreted 'transformation' factors have been shown to caudalize neural tissue in whole embryos or explants: retinoic acid (Durston et al., 1989; Sive et al., 1990; Ruiz i Altaba and Jessell, 1991; Sharpe, 1991; Kolm and Sive, 1995; Papalopulu, and Kintner, 1996; Godsave et al., 1998), basic fibroblast growth factor (bFGF; Kenkgaku and Okamato, 1995; Lamb and Harland, 1995; Cox and Hemmati-Brivanlou, 1995) and Xwnt3a (McGrew et al., 1995; McGrew et al., 1997). These factors and/or their receptors are expressed in the neural plate in a temporal and regional manner, supporting their roles as caudalizers of the nervous system. All three of these molecules caudalize in non-equivalent manners and it is still not clear how they interact to specify proper AP pattern in the CNS (Kolm et al., 1997; rev. in Gamse and Sive, 2000).

In *Xenopus* embryos and explants, Meis homeobox proteins have been shown to caudalize and dorsalize the CNS (Salzberg et al., 1999; Maeda et al., 2001). The caudalizing *Xenopus Meis3* gene (Salzberg et al., 1999) was originally identified as a *Drosophila homothorax* (*hth*) gene homolog (Rieckhof et al., 1997; Kurant et al., 1998). In neurula embryos, *XMeis3* is

expressed in the hindbrain from rhombomere 2 (r2) to rhombomere 4 (r4), and in the anterior spinal cord (Salzberg et al., 1999). Ectopic *XMeis3* expression in embryos causes anterior truncations, with a loss of anterior neural tissues from the cement gland/forebrain until the midbrain-hindbrain junction. In parallel, hindbrain and spinal cord cell types are expanded in embryos that overexpress *XMeis3*. Expression of pan-neural markers is unaltered by ectopic *XMeis3* expression.

In neuralized animal cap explants, ectopic *XMeis3* expression inhibits anterior neural induction by BMP antagonists such as noggin or the BMP2/4 dominant-negative (DN) receptor; however, XMeis3 does not inhibit the ability of these BMP antagonists to induce pan-neural markers (Salzberg et al., 1999). Strikingly, in naïve animal cap ectoderm, ectopic *XMeis3* expression induces transcriptional activation of hindbrain and spinal cord neural markers, albeit in the absence of pan-neural marker expression (Salzberg et al., 1999). This effect is ectoderm-specific, as XMeis3 does not activate transcription of mesodermal markers in injected animal cap explants (Salzberg et al., 1999). Thus, the XMeis3 protein 'uncouples' neural caudalization from neural induction.

To further examine the role of XMeis3 protein in *Xenopus* neural development, two distinct strategies have been used to inhibit endogenous XMeis3 protein activity. In the first strategy, fusions of a XMeis3 open reading frame to either the *Engrailed* transcriptional repressor domain or the *VP16* transcriptional activation domain were compared in embryos and explants. We found that the Eng-XMeis3 fusion protein acted as an antimorph, blocking the effects of wild-type *XMeis3*-encoding RNA in *Xenopus* embryos and explants, while the VP16-XMeis3 fusion protein acted as a transcriptional activator to caudalize embryos and explants. In embryos, ectopic XMeis3-antimorph (XMeis3-AM) protein expression caused a loss of hindbrain marker expression, with a concomitant posterior expansion of anterior neural markers into the hindbrain region. Spinal cord and pan-neural marker expression was unaltered by the XMeis3-AM protein. In a second experimental approach, inhibition of *XMeis3* mRNA translation by injection of XMeis3 antisense morpholino oligonucleotides (AMOs) also disrupted *Xenopus* hindbrain formation.

In animal cap explants caudalized by bFGF or Wnt3a, antagonism of XMeis3 protein activity did not specifically inhibit caudalizer activity, but it did rostralize the AP extent of posterior neural marker expression. XMeis3 activity is probably required for cells to overcome anterior neural signaling, thus enabling proper hindbrain cell fate identity in the developing *Xenopus* CNS.

MATERIALS AND METHODS

Construction of XMeis3-antimorph constructs

Two sets of Eng-XMeis3 and VP-XMeis3 fusion proteins were constructed. In the first set, PFU DNA polymerase (Promega) generated full-length fragments (amino acids 1-385) that were cloned in frame 3′ to the *VP16* or *Engrailed* domains in the pCS2 vector (Kessler, 1995). In the second set of constructs, the region spanning amino acids 1-333 was cloned in the same manner. These latter two constructs contain the Meis homology-box and homeodomain regions, but lack all of the region C-terminal to the homeodomain. All four of these constructs were subcloned into the pSP64T+globin

vector. Both sets of Eng-XMeis3 constructs acted as antimorphs; the shorter version was more effective and was used in the shown experiments. Both sets of VP-XMeis3 constructs acted as caudalizers; the longer version was more effective and was used in the shown experiments.

Xenopus embryos, explants and inducing factors

Ovulation, in vitro fertilization, embryo culture and dissections were carried out as described by Re'em-Kalma et al. (Re'em-Kalma et al., 1995). Embryos were staged according to Nieuwkoop and Faber (Nieuwkoop and Faber, 1967). *Xenopus* bFGF (XbFGF) treated (50 ng/ml) animal cap explants were cultured as described by Lamb and Harland (Lamb and Harland, 1995).

RNA injections

Different concentrations of capped sense in vitro transcribed full-length *XMeis3* (Salzberg et al., 1999)*, Eng-XMeis3* and *VP16-XMeis3* (0.1-1.8 ng in a volume of 5-10 nl) were injected into the animal hemisphere of embryos at the one or two-cell stages. Capped in vitro transcribed *Xenopus noggin* RNA (200 pg) and mouse *Wnt3a* RNA (100 pg) were injected into the animal hemisphere of embryos at the one-cell stage (Smith and Harland, 1992; Baker et al., 1999).

Injection of antisense morpholino oligonucleotides (AMOs)

Antisense morpholino oligonucleotides (AMOs) complementing the 5′ region of the *XMeis3* mRNA were designed by and purchased from Gene Tools, LLC; Corvallis, OR (www@gene-tools.com; Heasman et al., 2000; Nasevicius and Ekker, 2000). The *XMeis3* AMO sequence is 5′-ATACCTTTGTGCCATTCCGAGTTGG-3′. A standard control morpholino oligonucleotide (CMO) was also used in each experiment (Gene Tools). AMOs and CMOs were dissolved at 2 mg/ml in sterile water. One-cell embryos were routinely injected in the 10-20 ng range in 5-10 nl volumes. In two-cell stage embryos, one blastomere was injected with 7.5 ng in a 5 nl volume. The AMO was toxic at levels above 30 ng/embryo and experiments were performed at significantly lower concentrations.

In situ hybridization

Whole-mount in situ hybridization was carried out with digoxigenin-labeled probes, as described previously (Hemmati-Brivanlou et al., 1990; Harland, 1991; Knecht et al., 1995). Double in situ hybridization experiments were performed with probes generated from fluorescein and digoxigenin RNA-labeling mixes (Roche). Embryos were stained with BM purple and Fast Red substrates (Roche; Hollemann et al., 1998). In some cases, both probes were stained with BM purple. Two-cell stage albino embryos were injected unilaterally into the animal hemisphere of one-cell with 50-100 pg of RNA encoding the XMeis3-AM protein or 6-7.5 ng of the AMO. Embryos were cultured until late neurula stages and subsequently fixed for in situ hybridization. The uninjected side served as an internal control in all experiments. For lineage tracing analysis, 50 pg of RNA encoding the β-galactosidase protein (β-gal; Smith and Harland, 1991) and RNA encoding the XMeis3-AM protein were co-injected unilaterally at the two-cell stage. Embryos were stained in red for β-gal activity and fixed for whole-mount in situ hybridization as described previously (Bonstein et al., 1998). The perturbations seen in the embryos were always seen on the red stained β-gal/XMeis3-AM or AMO injected side (data not shown).

RT-PCR analysis

RT-PCR was performed as described previously (Wilson and Melton, 1994), except that random hexamers (100 ng/reaction) were used for reverse transcription. Primers for *EF1α*, *En2*, *Krox20* and *HoxB9* have been described elsewhere (Hemmati-Brivanlou and Melton, 1994). The primers for *HoxD1* and *RARα2.2* have been described by Kolm et al. (Kolm et al. 1997). The *otx2* and *XAG1* primers are described

elsewhere (Knecht et al., 1995). The *XE10* primers are described elsewhere (Weinstein et al., 1996). The *HoxB3* primers have been described by Hooiveld et al. (Hooiveld et al., 1999).

Western blot analysis

Western blot analysis was performed as described (Henig et al., 1998). For constructing the XMeis3-Myc vector, a full-length XMeis3 PFU generated fragment was subcloned 5′ to the Myc fusion site in the pCS2+MT vector. This plasmid was linearized with *Not*I and transcribed with Sp6 to generate RNA encoding XMeis3-Myc fusion protein. XMeis3-Myc RNA (1.6 ng) was co-injected with 16 ng of XMeis3-AMO or CMO into one-cell stage embryos. Protein was isolated from a pool of ten embryos per group at stage 12.5. A total of 50 µg protein was loaded per sample for electrophoresis. Western blot analysis was performed using the 9E10 Myc antibody. As a control for protein loading, total Erk protein was detected by the p44/p42 antibody (New England Biolabs). As a positive control, in vitro transcribed/translated Meis3-Myc protein (TNT system; Promega) was loaded for electrophoresis.

RESULTS

ENG-XMeis3 protein antagonizes XMeis3 caudalizing activity in contrast to VP16-XMeis3 protein

To inhibit XMeis3 protein activity during early development, we constructed an XMeis3 antimorph protein by fusing two different XMeis3 open reading frames (see Materials and Methods) to either the *Engrailed* (*ENG*) transcriptional repressor domain or the *VP16* transcriptional activator domain (Fig. 1). In a relatively simple animal cap explant assay, antimorph candidate RNA molecules were screened by co-injection with wild-type *XMeis3*-encoding RNA (Fig. 2A-B). *XMeis3* RNA activates expression of a panel of posterior neural markers in animal cap ectoderm (Salzberg et al., 1999); thus, any bona fide antimorph-encoding RNA should antagonize wild-type XMeis3 protein caudalizing activity in co-injected animal cap explants.

Co-injection of RNA encoding the ENG-XMeis3 chimera protein inhibited wild type XMeis3 caudalization activity in animal caps (Fig. 2A). As expected, *XMeis3* activated *Krox20*, *HoxD1* and *HoxB9* expression in animal caps (Fig. 2A, lane 4), whereas injection of *XMeis3-AM* alone did not transcriptionally activate these markers (Fig. 2A, lane 5). However, in the *XMeis3*/*XMeis3-AM* co-injected group, posterior neural marker expression was eliminated (Fig. 2A, compare lane 4 with lane 6). By contrast, injection of RNA encoding the VP16-XMeis3 chimera protein induced posterior neural marker transcription in animal cap explants (Fig. 2B, compare lane 4 with lane 3). Ectopic *VP16-XMeis3* expression
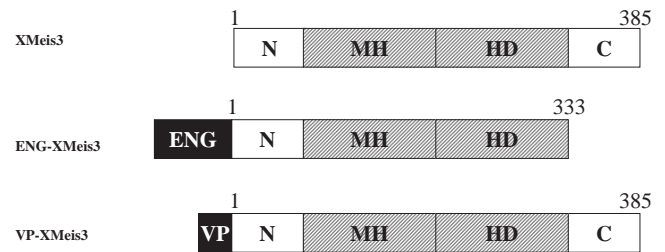

Fig. 1. Fusion constructs used for expression in *Xenopus* tissue (see Materials and Methods). (Top) Wild-type full-length XMeis3 protein. (Middle) Eng-XMeis3/XMeis3-antimorph protein. (Bottom) VP-XMeis3 activator protein.

caused anterior truncations in whole embryos (Fig. 2C); this is the same phenotype observed in embryos ectopically expressing wild-type *XMeis3* RNA (Salzberg et al., 1999). These results suggest that XMeis3 protein may act as a transcriptional activator in the embryo to induce posterior neural gene expression.

Ectopic *XMeis3-antimorph (XMeis3-AM)* expression eliminates the hindbrain region and expands anterior neural tissues

To address the role of endogenous XMeis3 protein in early development, we injected 400-800 pg of in vitro synthesized *XMeis3* antimorph (*XMeis3-AM*) -encoding RNA into the animal hemisphere of one-cell *Xenopus* embryos. Embryos were scored at tailbud to tadpole stages for phenotypes (Fig. 2D). Overexpression of *XMeis3*-AM RNA caused anterior expansions in over 80% (n=40/48) of the injected embryos in the shown experiment. In comparison with control embryos, these embryos had enlarged cement glands and a shortened body axis (Fig. 2D).

To further examine the effects of ectopic *XMeis3*-AM expression on spatial expression of neural markers, whole-mount in situ hybridization was performed on *XMeis3-AM*-injected late neurula stage embryos. Embryos were unilaterally injected (50-100 pg of *XMeis3-AM* RNA) into the animal hemisphere of one blastomere at the two-cell stage. Complementing the observation of cement gland expansion (Fig. 2D), in nearly 60% of *XMeis3-AM* injected embryos (n=33/56), expression of the forebrain/midbrain-specific *otx2* (Blitz and Cho, 1995) and forebrain-specific *cpl-1* (Knecht et al., 1995) markers was posteriorly expanded (Fig. 3A-D). As seen in the double in situs with *Krox20* or *En2*, *otx2* expression was dramatically expanded into the hindbrain region (Fig. 3B-C). In the most extreme phenotypes, *otx2* expression extended

Table 1. Ectopic XMeis3-antimorph action on neural marker expression

Gene analyzed	Number of embryos with modified gene expression on injected side	Number of embryos with unchanged gene expression on injected side
En2	48/67 (76%)	19/67 (24%)
Krox20	38/50 (76%)	12/50 (24%)
XE10	22/22 (100%)	0
HoxB1	7/12(58%)	5/12 (42%)
HoxB3	28/38 (74%)	10/38 (26%)
HoxB9	1/22 (5%)	21/22 (95%)
n-tubulin	13/13 (100%)	0
Nrp1	0	13/13 (100%)

Fig. 2. *Eng-XMeis3* RNA encodes an antimorph protein; *VP16-XMeis3* RNA encodes a caudalizing protein. (A) One-cell stage embryos were injected in the animal hemisphere with 1.0 ng of *XMeis3* RNA (lane 4), 1.6 ng of *Eng-XMeis3* RNA (*XMeis3-AM*; lane 5) or both (lane 6). Eighteen animal cap explants were removed from uninjected (lane 3) and injected groups (lanes 4-6) of blastula embryos (stage 8-9). Explants from each group were grown to stage 20 and total RNA was isolated. RT-PCR analysis was performed with the markers: *Krox20*, *HoxD1 and HoxB9*. *EF1α* served as a control for quantifying RNA levels in the different samples. For controls, RT-PCR (lane 2) and −RT-PCR (lane 1) were performed on total RNA isolated from normal embryos. (B) One-cell stage embryos were injected in the animal hemisphere with 1.6 ng of *VP16-XMeis3* RNA (lane 4). Eighteen animal cap explants were removed from uninjected (lane 3) and injected groups (lane 4) of blastula embryos (stage 8-9). Explants from each group were grown to stage 20 and total RNA was isolated. RT-PCR analysis was performed with the markers: *Krox20*, *HoxB3*, *HoxD1 and RARα2.2*. *EF1α* served as a control for quantifying RNA levels in the different samples. For controls, RT-PCR (lane 2) and −RT-PCR (lane 1) were performed on total RNA isolated from normal embryos. (C) Embryos at the one-cell stage were injected with 1.3 ng of in vitro transcribed *VP16-XMeis3*. The upper embryo serves as an uninjected control. Injected embryos had anterior truncations and highly reduced cement gland formation (lower panel). The dorsal anterior index (DAI, Kao and Elinson, 1988) was 2.5 (*n*=39); over 20% of the embryos completely lacked cement glands and another 80% had extreme posterior truncations, with partial cement gland formation (lower panel). Embryos are oriented posterior to anterior: left to right. Embryos were fixed for photography at stages 35/36. (D) Embryos at the one-cell stage were injected with 1.0 ng of *XMeis3-AM* antimorph RNA. The top embryo serves as an uninjected control. In this representative experiment, over 80% of the *XMeis3-AM* injected displayed phenotypes. Embryos are oriented posterior to anterior: left to right. Embryos were fixed for photography at stages 30/31.
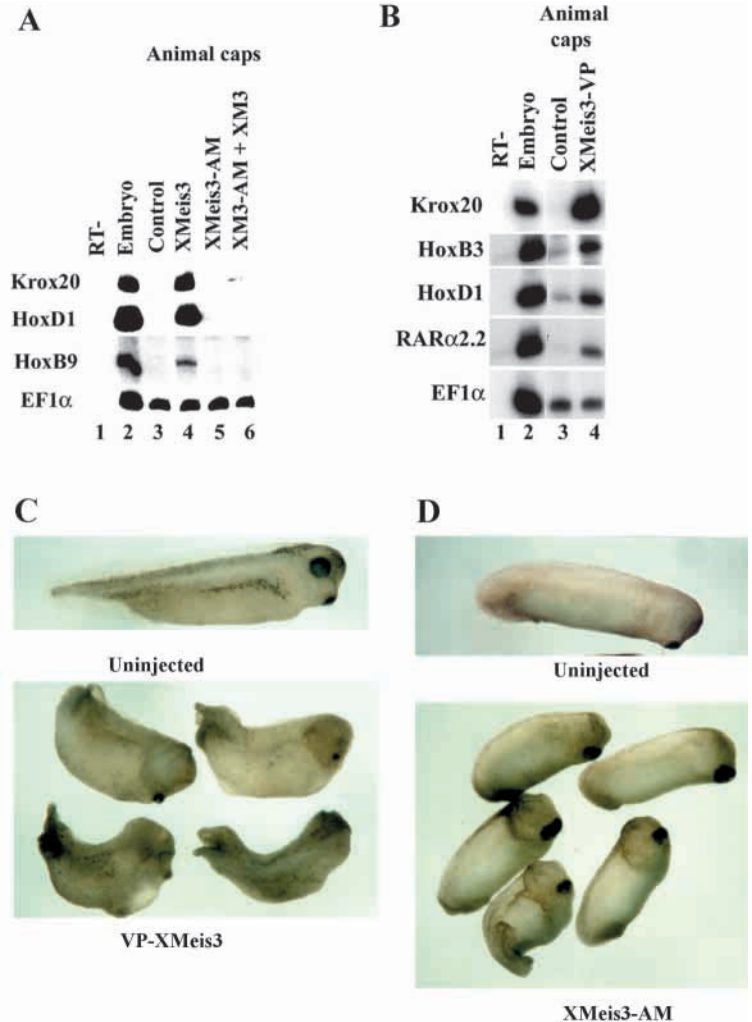
posteriorly into the r4/r5 boundary (Fig. 3B). *cpl-1* expression was also shifted into the hindbrain region, as shown by the double in situ with *En2* (Fig. 3D). In the cement gland, *XAG1* and *XA1* (not shown) expression (Sive et al., 1989) spread posteriorly in over 60% of the embryos (*n*=25/40). *XAG1* expression appeared to extend into both spinal cord and lateral epidermal regions (Fig. 3E).

Hindbrain marker expression was severely inhibited in *XMeis3-AM*-injected embryos. *Krox20* (Bradley et al., 1992) expression in r3/r5 was reduced in over 75% of the injected embryos (Fig. 3G,B,K-M; Table 1). In the mildest of phenotypes, r3/r5 expression is pushed posteriorly into r5/r7 (Fig. 3K). Rhombomere 4-specific markers, such as *XE10* (Weinstein et al., 1996) and *HoxB1* (Godsave et al., 1998) were also highly reduced in *XMeis3-AM*-injected embryos (Fig. 3H-I; Table 1). Interestingly, *HoxB3* (Godsave et al., 1998) expression in r5/r6 was also eliminated, yet *XMeis3* is not expressed at high levels in these rhombomeres (Fig. 3J; Table 1).

En2 (Hemmati-Brivanlou and Harland, 1989) expression was altered in the mid-hindbrain junction in over 75% of the *XMeis3-AM*-injected embryos (Table 1). However, the perturbed expression of *En2* was of a more subtle nature in comparison with hindbrain markers. In embryos displaying the most moderate XMeis3-AM phenotypes, we did not observe major reductions in *En2* expression, but expression expanded as far as r3/r4 (Fig. 3C,K). In intermediate phenotypes, we observed a posterior spreading of *En2* to r2/r3 with a concomitant loss of *Krox20* expression (Fig. 3L). In more extreme phenotypes, *En2* expression was lost, together with *Krox20* (Fig. 3M,D).

Expression of the pan-neural *nrp1* marker (Fig. 3F; Table 1; Richter et al., 1988) and the spinal cord-specific *HoxB9* marker (Fig. 3G; Table 1; Wright et al., 1990) was unaltered by ectopic *XMeis3-AM* expression, despite overlapping *XMeis3* mRNA expression in the hindbrain and anterior spinal cord (Salzberg et al., 1999). Interestingly, expression of the neuron specific *n-tubulin* marker (Hollemann et al., 1998) was highly inhibited (Fig. 3N; Table 1) by ectopic XMeis3-AM activity. In strong phenotypes, both the r2-derived trigeminal neuron as well as the more posterior neural expression was eliminated. In more moderate phenotypes, the trigeminal was still missing but posterior expression was less inhibited (not shown). Thus, *XMeis3* may have a role in early neuron specification.

These results demonstrate that ectopic *XMeis3-AM* expression can cause an anterior transformation of the hindbrain by inhibiting caudalization. Thus, functional XMeis3
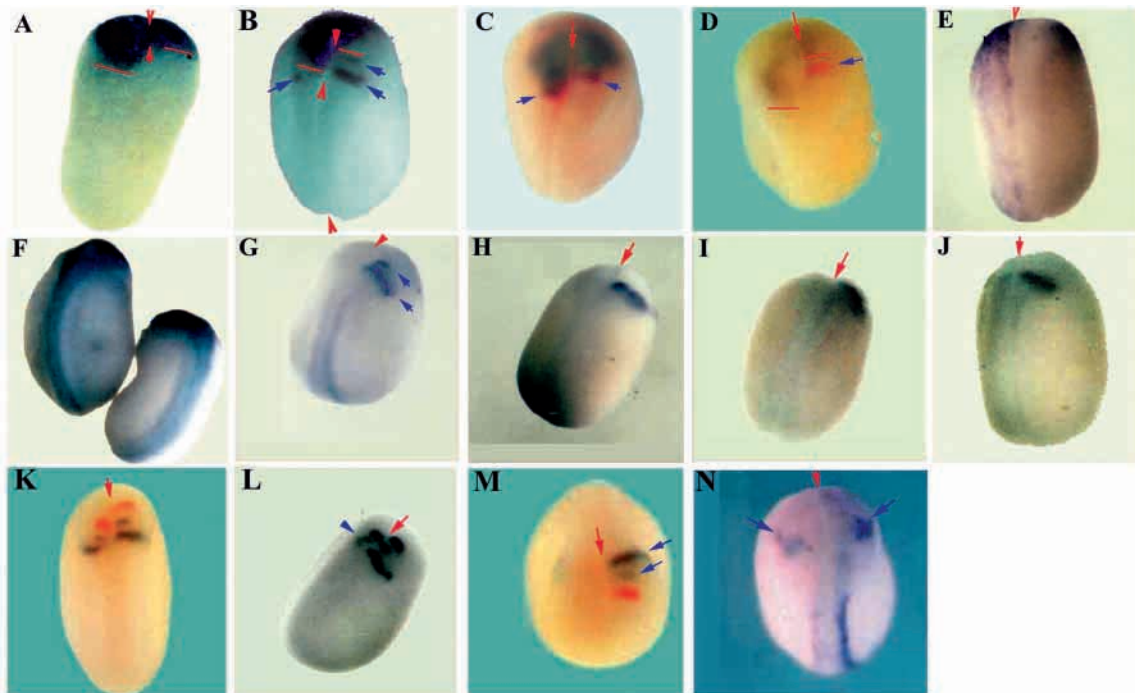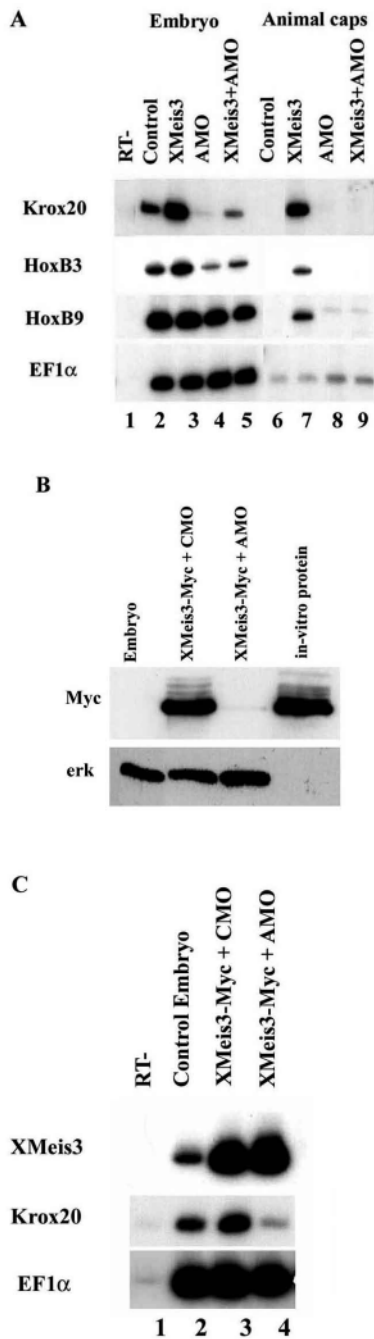
Fig. 3. Expression pattern of neural markers in embryos injected with *XMeis3-AM* RNA. Two-cell albino embryos were injected unilaterally into the animal hemisphere of one blastomere with 50-100 pg of *XMeis3*–AM RNA. The red arrow delineates the dorsal midline. In all embryos, *XMeis3-AM* injection is on the left side. In all cases (except Fig. 3M), embryos are viewed dorsally; embryos are oriented anterior (top) to posterior (bottom). (A) In situ hybridization with *otx2*. Expression is expanded posteriorly on the *XMeis3-AM* injected side. The red lines delineate the AP extent of *otx2* expression on the uninjected versus injected side. (B) In situ hybridization with *otx2* and *Krox20*. *otx2* expression is expanded posteriorly and *Krox20* expression (blue arrows) is lost on the *XMeis3-AM*-injected side. The red lines delineate the AP extent of *otx2* expression on the uninjected versus injected side. (C) In situ hybridization with *otx2* and *En2* (red). Expression of *o*tx2 and *En2* (blue arrows) is expanded posteriorly. (D) In situ hybridization with *cpl-1* and *En2* (red). *cpl-1* expression is expanded posteriorly and *En2* expression (blue arrow/uninjected side) is lost on the *XMeis3-AM*-injected side. The red lines delineate the AP extent of *cpl-1* expression on the uninjected versus injected side. (E) In situ hybridization with *XAG1*; expression is expanded posteriorly and laterally on the *XMeis3-AM* injected side. (F) In situ hybridization with *nrp1*; expression is unchanged on the *XMeis3-AM* injected side. (G) In situ hybridization with *Krox20* and *HoxB9*; *Krox20* expression (blue arrows/uninjected side) is eliminated on the *XMeis3-AM*-injected side. HoxB9 expression is unchanged on the *XMeis3-AM* injected side. (H) In situ hybridization with *XE10*. *XE10* expression is eliminated on the *XMeis3-AM*-injected side. (I) In situ hybridization with *HoxB1*. *HoxB1* expression is eliminated on the *XMeis3-AM* injected side. (J) In situ hybridization with *HoxB3*. *HoxB3* expression is eliminated on the *XMeis3-AM*-injected side. (K) In situ hybridization with *En2* (red) and *Krox20*. *En2* expression is pushed posteriorly to the r3/r4 boarder and *Krox20* expression is pushed posteriorly to the r5/r7 boarder on the *XMeis3-AM*-injected side. (L) In situ hybridization with *En2* and *Krox20*. *En2* expression is pushed posteriorly to r3 on the *XMeis3-AM*-injected side. The blue arrow delineates the reduced *Krox20* expression (fused stripes) on the injected side. (M) In situ hybridization with *En2* (red) and *Krox20*. Expression of *En2 and Krox20* (blue arrows/uninjected side) is eliminated on the *XMeis3-AM*-injected side. An anterior view of the embryo: dorsal (top) to ventral (bottom). (N) In situ hybridization with *n-tubulin*. *n-tubulin* expression is eliminated on the *XMeis3-AM*-injected side. The trigeminal neuron is marked by blue arrows on both sides.

protein appears to be required for correct specification of the hindbrain in early *Xenopus* development.

Antisense morpholino oligonucleotides also inhibit XMeis3 caudalizing activity and hindbrain pattern

An additional molecular tool for antagonism of in vivo XMeis3 protein activity is antisense morpholino oligonucleotides (AMOs). AMOs have recently been shown to inhibit mRNA translation in *Xenopus* and zebrafish embryos (Heasman et al., 2000; Nasevicius and Ekker, 2000). AMOs, complementary to the 5′ UTR and spanning the initial translated codons of the *XMeis3* mRNA (see Materials and Methods) were injected at the one-cell stage into the animal hemisphere of embryos. In every experiment, a control morpholino oligonucleotide (CMO) was injected at an identical concentration to the AMO (see Materials and Methods). As described previously for

XMeis3-AM, the specific inhibitory effect of AMOs on XMeis3 activity was screened by co-injection with wild-type *XMeis3* RNA. Injection of *XMeis3* AMOs together with *XMeis3* wild-type RNA inhibited caudalizing activity in both animal cap explants and whole embryos (Fig. 4A). In animal cap explants, *XMeis3* ectopically activated expression of the *Krox20*, *HoxB3* and *HoxB9* genes (Fig. 4A, lane 7), but in explants co-expressing *XMeis3* and the AMO, posterior neural marker expression was eliminated (Fig. 4A, lane 9). In whole embryos, ectopic XMeis3 significantly increased *Krox20* and *HoxB3* gene expression (Fig. 4A, lane 2); this increase was inhibited by co-expression with the AMO (Fig. 4A, lane 5). Strengthening this observation, expression of the AMO in embryos significantly reduced normal *Krox20* and *HoxB3* expression levels, in comparison with CMO-injected control embryos (Fig. 4A, compare lanes 2 and 4). *HoxB9* expression

A

Embryo   Animal caps

RT-
Control
XMeis3
AMO
XMeis3+AMO
Control
XMeis3
AMO
XMeis3+AMO

Krox20

HoxB3

HoxB9

EF1α

1   2   3   4   5   6   7   8   9

B

Embryo
XMeis3-Myc + CMO
XMeis3-Myc + AMO
in-vitro protein

Myc

erk

C

RT-
Control Embryo
XMeis3-Myc + CMO
XMeis3-Myc + AMO

XMeis3

Krox20

EF1α

1   2   3   4

Fig. 4. *XMeis3* antisense morpholino oligonucleotide (AMO) inhibits posterior neural marker expression by blocking translation of *XMeis3* RNA. (A) One-cell stage embryos were injected in the animal hemisphere with 15 ng of AMO (lanes 4-5 and 8-9), 15 ng of control morpholino oligonucleotide (CMO; lanes 2-3 and 6-7) and 1.0 ng of *XMeis3* RNA (lanes 3, 5, 7 and 9). Eighteen animal cap explants were removed from all injected groups (lanes 6-9) of blastula embryos (stage 8-9). Explants from each group were grown to stage 20 and total RNA was isolated. In parallel, total RNA was also isolated from pools of seven embryos from each injected group (lanes 1-5). RT-PCR analysis was performed with the markers: *Krox20*, *HoxB3* and *HoxB9*. *EF1α* served as a control for quantifying RNA levels in the different samples. For controls, RT-PCR (lane 2) and −RT-PCR (lane 1) were performed on total RNA isolated from normal CMO-injected embryos (lane 2). (B) Western analysis of XMeis3-Myc protein. One-cell stage embryos were injected in the animal hemisphere with 1.6 ng of RNA encoding the XMeis3-Myc fusion protein (lanes 2-3) and 16 ng of AMO (lane 3) or 16 ng of CMO (lane 1-2). Protein was isolated from pools of seven embryos per group at stage 12.5: control (lane 1), XMeis3-Myc/CMO (lane 2), XMeis3-Myc/AMO (lane 3). As a positive control, in vitro synthesized XMeis3-Myc protein was also examined on the filter (lane 4). Analysis was performed using the 9E10 Myc antibody. As a positive control, total Erk protein was detected with the p44/p42 antibody. (C) Embryos from the above experiment (Fig. 4B) were grown to late neurula stages. Total RNA was also isolated from pools of seven embryos from the control (lanes 1-2) and injected groups (lanes 3-4). RT-PCR analysis was performed with the markers *XMeis3* and *Krox20*. *EF1α* served as a control for quantifying RNA levels in the different samples. For controls, RT-PCR (lane 2) and −RT-PCR (lane 1) were performed on total RNA isolated from uninjected control embryos (lane 2).

was not disrupted in AMO-injected embryos (Fig. 4A, lanes 2-5).

To demonstrate that the AMO was indeed inhibiting translation of *XMeis3* RNA, the AMO was co-injected with RNA encoding a XMeis3-Myc-tagged protein. As determined by Western blot analysis, co-injection of AMO prevented translation of this XMeis3-Myc tagged protein in comparison with embryos co-injected with the CMO (Fig. 4B, compare lanes 2 and 3). The effects on XMeis3-Myc translational inhibition were specific, as AMO and CMO injections did not inhibit endogenous *Xenopus* proteins; Erk levels were identical in all groups (Fig. 4B, compare lanes 1-3). In contrast to protein levels, the AMO did not alter XMeis3-Myc RNA
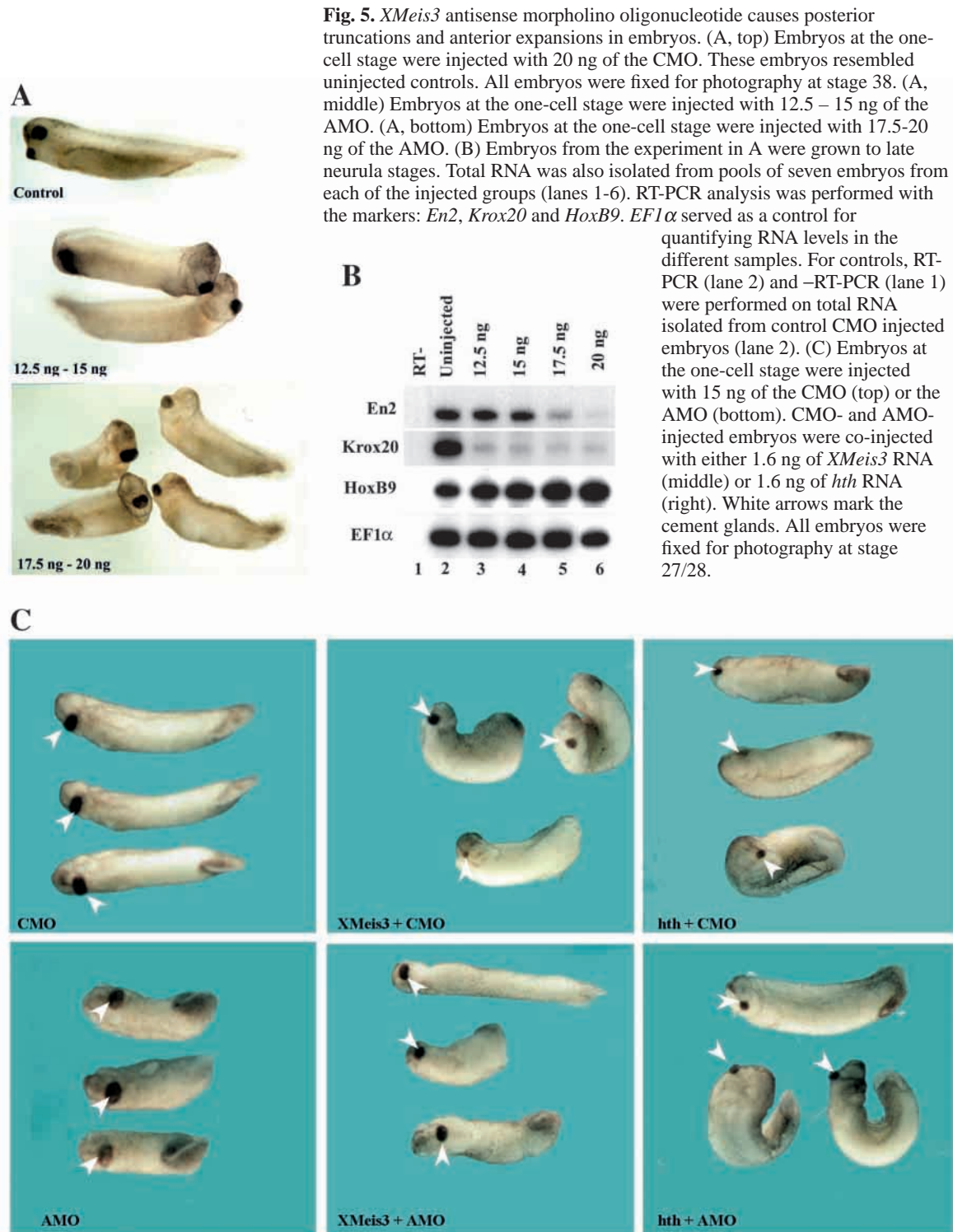
levels, as RNA levels were identical in the AMO- and CMO-injected groups (Fig. 4C, compare lanes 1 and 2).

In XMeis3-Myc/CMO-injected embryos, XMeis3-Myc protein acts as a caudalizer, increasing Krox20 expression in these embryos (Fig. 4C, compare lanes 2 and 3). However, when XMeis3-Myc/AMO was co-injected, levels of Krox20 RNA were highly reduced, significantly below levels in control embryos (Fig. 4C, lanes 2-4).

To further determine the role of endogenous XMeis3 protein in the embryo, we used the AMO to inhibit endogenous *XMeis3* mRNA translation during early development. We injected 12.5-20 ng of the AMO into the animal hemisphere of one-cell stage embryos; these embryos were scored at tailbud to tadpole stages for phenotypes (Fig. 5). Like ectopic *XMeis3-AM* expression, the AMO (17.5-20 ng) caused anterior expansions and cement gland enlargement in over 80% (*n*=41/49) of the injected embryos (Fig. 5A, lower panel), in comparison with control CMO-injected embryos (Fig. 5A, upper panel). As in the case of the XMeis3-AM phenotypes, these embryos also had a much shorter body axis; body length was reduced by approximately 25-33% in AMO phenotypic embryos. At lower AMO concentrations (12.5-15 ng), body length was still altered in over 75% of the embryos (*n*=37/54), and anterior expansion phenotypes were weaker (Fig. 5A, middle panel). Thus, like the XMeis3-AM protein, injection of the AMO caused a prominent dose-dependent anteriorized phenotype in embryos.

By RT-PCR analysis, neural marker expression was examined over the 12.5-20 ng AMO concentration range (Fig. 5B). *Krox20* expression is the most sensitive to loss of XMeis3

Fig. 5. *XMeis3* antisense morpholino oligonucleotide causes posterior truncations and anterior expansions in embryos. (A, top) Embryos at the one-cell stage were injected with 20 ng of the CMO. These embryos resembled uninjected controls. All embryos were fixed for photography at stage 38. (A, middle) Embryos at the one-cell stage were injected with 12.5 – 15 ng of the AMO. (A, bottom) Embryos at the one-cell stage were injected with 17.5-20 ng of the AMO. (B) Embryos from the experiment in A were grown to late neurula stages. Total RNA was also isolated from pools of seven embryos from each of the injected groups (lanes 1-6). RT-PCR analysis was performed with the markers: *En2*, *Krox20* and *HoxB9*. *EF1α* served as a control for quantifying RNA levels in the different samples. For controls, RT-PCR (lane 2) and −RT-PCR (lane 1) were performed on total RNA isolated from control CMO injected embryos (lane 2). (C) Embryos at the one-cell stage were injected with 15 ng of the CMO (top) or the AMO (bottom). CMO- and AMO-injected embryos were co-injected with either 1.6 ng of *XMeis3* RNA (middle) or 1.6 ng of *hth* RNA (right). White arrows mark the cement glands. All embryos were fixed for photography at stage 27/28.

activity, being highly reduced at all concentrations examined (Fig. 5B). *HoxB3* expression was also inhibited (not shown). *En2* expression is lost, but in a graded manner and only at higher AMO concentrations (Fig. 5B). *HoxB9* expression was not reduced, being slightly increased in AMO-injected embryos (Fig. 5B). Expression levels of the ectodermal and mesodermal markers, *epidermal cytokeratin* and *muscle actin* were not significantly altered by the AMOs (not shown).

To demonstrate AMO specificity, *XMeis3* and *Drosophila hth*-encoding RNAs were separately co-injected into embryos together with the AMO. We have previously shown that ectopic *hth* expression can caudalize *Xenopus* embryos and animal cap explants, in the same way as *XMeis3* (Salzberg et al., 1999). As the *hth* gene lacks the *XMeis3* 5′ region encoded by the AMO, we expect that its caudalizing activity should not be affected by the AMO. Indeed, both RNAs caudalized embryos

Fig. 6. *XMeis3* antisense morpholino oligonucleotide eliminates hindbrain marker expression. Two-cell albino embryos were injected unilaterally into the animal hemisphere of one blastomere with 6-7.5 ng of the *XMeis3* AMO. In situ hybridization was performed in late neurula stage embryos. In all cases, embryos are viewed dorsally; embryos are oriented anterior (top) to posterior (bottom). The red arrow delineates the dorsal midline. Embryos were injected on the right side. (A) In situ hybridization with *Krox20* and *HoxB9*; *Krox20* expression is eliminated on the AMO-injected side. *HoxB9* expression is unchanged on the AM- injected side. (B) In situ hybridization with *XE10*; expression is eliminated on the AMO-injected side. (C) In situ hybridization with *HoxB3* and *HoxB9*; *HoxB3* expression is eliminated on the AMO-injected side. *HoxB9* expression is unchanged on the AMO-injected side. (D) In situ hybridization with *XMeis3* and *En2* (red); expression of both markers is posteriorized on the AMO-injected side. (E) In situ hybridization with *XMeis3*; expression is inhibited on the AMO-injected side. The *XMeis3* expression in r2 is indicated by arrows on both sides.
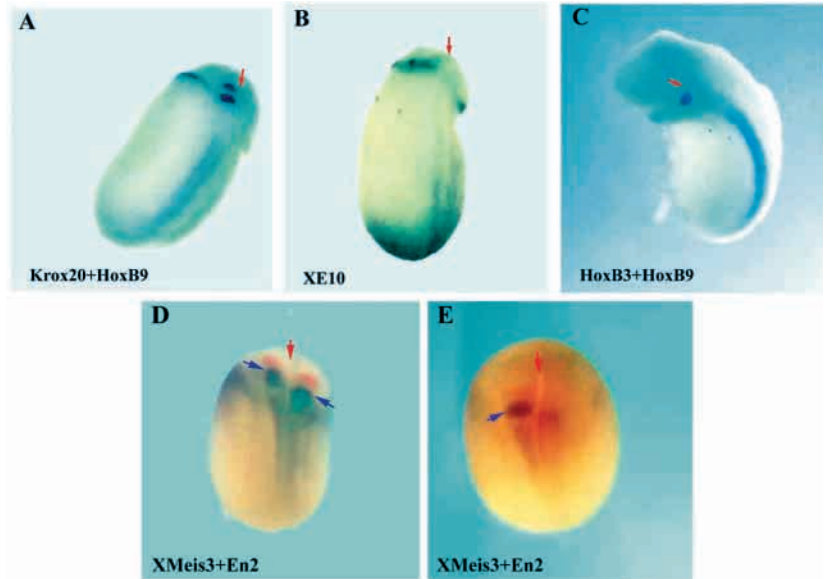
in a similar manner: 85% of the XMeis3/CMO injected embryos (*n*=8) and 75% of the hth/CMO (*n*=16) -injected embryos had small cement glands (Fig. 5C, upper panel). XMeis3/AMO-injected embryos had rescued caudalized phenotypes: nearly 80% of the embryos (*n*=18) had normal or expanded cement glands (Fig. 5C, lower panel). In sharp contrast, 70% (*n*=20) of the hth/AMO-injected embryos had small cement glands (Fig. 5C, lower panel), like the XMeis3/CMO-injected group (Fig. 5C, upper panel). In the AMO-injected control group, 75% (*n*=16) of the embryos had expanded cement glands (lower left panel), in comparison with the CMO-injected (upper left panel) group (*n*=10). Similar results were also seen in animal cap explants; expression of *Krox20* was reduced in XMeis3/AMO versus XMeis3/CMO-injected explants, but levels of *Krox20* expression were identical in hth/AMO- and hth/CMO-expressing explants (not shown). These results show that the AMO cannot inhibit *hth* caudalizing activity, thus, the AMO is indeed specific to the *XMeis3* gene.

To further examine the role of the AMO in neural patterning, whole embryos at the two-cell stage were injected unilaterally into one blastomere with 6-7.5 ng of AMO, and whole-mount in situ hybridization was performed. We saw a dramatic reduction in hindbrain marker expression on the injected side: *Krox20* (Fig. 6A), *XE10* (Fig. 6B) and *HoxB3* (Fig. 6C). *HoxB9* expression in the spinal cord was not decreased in AMO-injected embryos (Fig. 6A,C). In AMO-injected embryos, *XE10* expression was exclusively inhibited in the hindbrain (where *XMeis3* expression overlaps), but not in ectoderm regions found lateral to the neural tube, where *XMeis3* was not expressed (Fig. 6B). We also examined how AMO injection altered endogenous *XMeis3* expression in r2-r4 and the anterior spinal cord. In moderate phenotypes (Fig. 6D), we detected a shift of the *XMeis3* rhombomeric expression from r2-r4 to r5-r7 with a fusion of the expression domain to the spinal cord. In the same embryo, *En2* expression is pushed to the approximate r2/r3 boarder (Fig. 6D). In more extreme phenotypes (Fig. 6E), the *XMeis3* expression pattern is again shifted posteriorly, but *XMeis3* mRNA levels are also highly

reduced. These data strongly corroborate the results obtained with the XMeis3-AM protein (Fig. 3), providing substantial proof that XMeis3 protein activity is obligatory for proper cell fate determination in the hindbrain.

Caudalized animal caps: XMeis3-AM protein rostralizes AP coordinates

To elucidate specific XMeis3 interactions with caudalizing pathways, XMeis3-AM was ectopically expressed in animal caps caudalized by either *Xenopus* bFGF (XbFGF) or mouse Wnt3a proteins. At the one-cell stage, *XMeis3-AM*, *noggin* and/or mouse *Wnt3a* RNAs were injected in the animal hemisphere; at blastula stages animal cap explants were removed. In the experiments with XbFGF, animal caps were aged until stage 10.25, when XbFGF treatment was initiated (Lamb and Harland, 1995). Total RNA was isolated for RT-PCR analysis at late neurula stages.

In noggin-neuralized animal cap explants, XMeis3-AM protein modified caudalization by XbFGF and mouse Wnt3a. In these caps, the perturbation of XMeis3 activity did not inhibit caudalization per se, but did bias neural marker expression in a more anterior manner. In both noggin/XbFGF- and XbFGF-treated animal caps explants, XMeis3-AM protein decreased expression of spinal cord-specific *HoxB9* marker, yet increased expression of the more anterior *En2* marker (Fig. 7A). This effect was dependent on the initial AP coordinates of the explant. When caps are treated with XbFGF, only *HoxB9* is induced (Fig. 7A, lane 3), yet in the presence of the XMeis3-AM protein, both *HoxB9* (reduced levels) and *En2* are expressed (Fig. 7A, lane 4). In XbFGF/noggin-treated caps, both *En2* and *HoxB9* are expressed (Fig. 7A, lane 5); however, in the presence of XMeis3-AM protein, *En2* is exclusively expressed and at increased levels (Fig. 7A, lane 6). Thus, the final extent of anteriorization in the *XMeis3-AM* injected explants appears determined by the initial AP patterning coordinates in the explant that were pre-determined by FGF±noggin. The presence of the XMeis3-AM protein shifted neural marker expression in favor of the more anterior mid-hindbrain
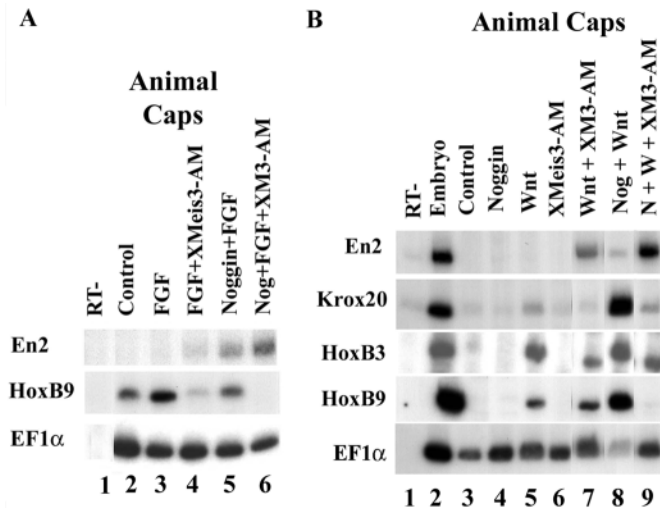
Fig. 7. XMeis3-antimorph protein anteriorizes neural marker expression in animal cap explants caudalized by bFGF or Wnt3a. (A) One-cell stage embryos were injected in the animal hemisphere with 1.6 ng of *XMeis3-AM* RNA (lane 4) or 0.2 ng of noggin RNA (lane 5) or both (lane 6). Eighteen animal cap explants were removed from uninjected (lanes 2-3) and injected groups of blastula embryos (stage 8-9). Explants from each group were aged until stage 10.25 and XbFGF was added at 50 ng/ml. Explants from each group were grown to late neurula stage and total RNA was isolated. RT-PCR analysis was performed with the markers: *En2* and *HoxB9*. *EF1α* served as a control for quantifying RNA levels in the different samples. −RT-PCR (lane 1) was performed on total RNA isolated from uninjected embryos. (B) One-cell stage embryos were injected in the animal hemisphere with 1.6 ng of *XMeis3-AM* RNA (lane 6-7 and 9), 0.2 ng of *noggin* RNA (lane 4 and 8-9) and/or 0.1 ng of mouse *Wnt3a* RNA (lanes 5, 7-9). Eighteen animal cap explants were removed from uninjected (lane 3) and injected groups of blastula embryos (stage 8-9). Explants from each group were grown to late neurula stage and total RNA was isolated. In parallel, total RNA was also isolated from uninjected control embryos (lanes 1-2). RT-PCR analysis was performed with the markers *En2*, *Krox20*, *HoxB3* and *HoxB9*. *EF1α* served as a control for quantifying RNA levels in the different samples. For controls, RT-PCR (lane 2) and −RT-PCR (lane 1) were performed on total RNA isolated from uninjected control embryos.

junction, while inhibiting expression of more posterior spinal cord and hindbrain markers.

Likewise, in noggin/Wnt3a-expressing animal caps, XMeis3-AM protein reduced levels of the *HoxB9*, *Krox20* and *HoxB3* markers, while it increased expression of the more anterior *En2* marker (Fig. 7B). The *Krox20*, *HoxB3* and *HoxB9* markers were induced to maximal levels in animal cap explants co-expressing ectopic *noggin* and mouse *Wnt3a* RNAs (Fig. 7B, lane 8). However in the animal cap explants expressing *XMeis3-AM*, *noggin* and mouse *Wnt3a*, *En2* expression was maximal, but *Krox20*, *HoxB3* and *HoxB9* expression levels were severely reduced (Fig. 7B, compare lanes 8 and 9).

In caps that solely expressed mouse *Wnt3a*, *XMeis3-AM* activated *En2* expression and inhibited hindbrain marker expression, but it did not inhibit *HoxB9* expression (Fig. 7B, compare lanes 5 and 7). In some instances, it even stimulated *HoxB9* expression (not shown).

DISCUSSION

We have used two experimental approaches to inhibit endogenous XMeis3 protein activity in developing *Xenopus* embryos. In the first approach, we constructed an antimorph protein, by fusing XMeis3 open reading frames to the *engrailed* repressor or *VP16* activator transcriptional domains. In the second approach, we injected an antisense morpholino oligonucleotide (AMO) homologous to the 5′ end of the *XMeis3* mRNA. In a relatively simple bioassay in animal cap explants, we determined that the Eng-XMeis3 fusion protein inhibited caudalizing activity when co-injected with wild-type *XMeis3* RNA. In the same animal cap assay, the VP16-XMeis3 fusion protein strongly activated expression of posterior neural markers. We thus concluded that the Eng-XMeis3 fusion protein acted as a bonafide antimorph protein.

Further supporting this observation, studies in transgenic flies that express either *Xenopus* Eng-XMeis3 or *Drosophila* Eng-HTH chimera proteins demonstrated *hth* loss-of-function like phenotypes (Inbal et al., 2001). In a complementary manner, transgenic flies expressing VP16-HTH chimera protein displayed *hth* gain-of-function like phenotypes; VP16-HTH also rescued phenotypes in *hth* mutant embryos (Inbal et al., 2001). Our previous studies demonstrated that ectopic expression of either wild-type HTH or XMeis3 proteins caudalized *Xenopus* embryos and animal cap explants (Salzberg et al., 1999). These results suggest that the Meis family transcriptional activator function has been conserved for nervous system development in such diverse organisms as flies and frogs.

Like the XMeis3-AM protein, injection of AMOs also inhibited wild-type XMeis3 caudalizing activity in embryos and animal cap explants. XMeis3-Myc protein levels were eliminated by the AMO. These results show that the AMO also acts as a potent inhibitor of XMeis3 activity, by preventing mRNA translation.

To address the role of XMeis3 during *Xenopus* CNS development, one-cell embryos were injected with the *ENG-XMeis3* (*XMeis3-AM*) RNA, *VP16-XMeis3* RNA or AMOs. Ectopic expression of VP16-XMeis3 RNA caudalized *Xenopus* embryos in a manner similar to the wild-type *XMeis3*-encoding RNA. By contrast, both *XMeis3-AM* and AMOs had distinct posterior-truncation/anterior-expansion phenotypes. In these embryos, the cement gland was expanded and the body axis was shortened.

To further address this point, albino embryos were unilaterally injected with *XMeis3-AM* or AMOs into one blastomere at the two-cell stage. At neurula stages, a wide array of neural markers were examined by whole-mount in situ hybridization. Confirming the phenotypic observations, in *XMeis3-AM*-injected embryos, we saw an expansion of expression of anterior markers such as *XAG1*, *cpl-1*, *otx2* and *En2* into more posterior regions of the brain. In the most extreme cases, we saw *otx2* expression shifted as far back as r4/r5 and *En2* expression was eliminated. In more moderate phenotypes, *otx2* expression was shifted to r1/r2 and *En2* expression was shifted to r3/r4. The posterior spread and loss of *En2* and endogenous *XMeis3* expression, and the concomitant loss of the r2-derived trigeminal neuron demonstrate that patterning in the most anterior hindbrain r1/r2 regions is greatly disrupted by the loss of endogenous XMeis3

activity. Rhombomeric expression of the *Krox20*, *XE10*, *HoxB1* and *HoxB3* markers was severely reduced by the XMeis3-AM protein or the AMO. In the most moderate hindbrain phenotypes, we could detect a two rhombomeric-shift of *Krox20* expression from r3/r5 to r5/r7. By contrast, the spinal cord and pan-neural markers, *HoxB9* and *nrp1* were unaffected by XMeis3-AM or AMO activity.

It also appears that neurogenesis may be affected by the loss of XMeis3 activity. In *XMeis3-AM* injected embryos, *n-tubulin* expression is always lost in the r2-derived trigeminal neuron, and this could be a reflection of rhombomeric identity loss in this region. In most cases, injection of the *XMeis3-AM* also inhibited posterior *n-tubulin* expression. Neither *XMeis3* nor *noggin* strongly induces *n-tubulin* expression in animal cap explants; however, in the presence of both molecules, we detected high levels of *n-tubulin* expression in animal caps (S. E. and D. F., unpublished). Thus, further experiments need to be performed to determine the exact role for XMeis3 protein in specifying neuron cell fates along the AP axis.

These results show that functional XMeis3 protein maintains a proper AP balance required for hindbrain formation. The spread of expression of anterior neural markers posteriorly into the hindbrain suggests that *XMeis3* is essential for actively maintaining a caudalized state in the hindbrain. While *XMeis3* does not seem required for neural induction, it seems to fine tune the AP pattern in the forebrain-hindbrain region. The conversion of hindbrain regions to more anterior fates, with concomitant posterior expansion of *XAG1*, *cpl-1*, *otx2* and *En2* expression emphasizes the role of XMeis3 in this AP fine-tuning process. *XMeis3* is expressed in the anterior spinal cord; however, it may not be required for proper spinal cord formation.

Animal cap assays shed an interesting light on the interactive role of XMeis3 with caudalizing signaling molecules such as XbFGF and Wnt3a, confirming a role for *XMeis3* as a neural patterning gene. Ectopic *XMeis3-AM* expression did not specifically inhibit caudalizing activity by these signaling molecules. However, the lack of XMeis3 activity did lead to a rostral shift in the AP levels of these explants that was dependent on the initial AP coordinates in the explants. In the case of animal cap explants treated solely with XbFGF, these caps expressed *HoxB9* but not *En2*; however, these explants expressed both *HoxB9* (reduced) and *En2*, when XMeis3 activity was inhibited. XbFGF/noggin-treated animal caps expressed both *HoxB9* and *En2*, yet in the presence of the XMeis3-AM, these caps ceased to express *HoxB9* and had increased levels of *En2*. Thus, in *XMeis3-AM*-expressing animal caps, the final AP output was determined by the initial AP status of the explant. XMeis3-AM protein shifted posterior neural marker expression to the anterior mid-hindbrain junction, while inhibiting expression of spinal cord and hindbrain markers. Our previous studies have shown that XMeis3 caudalization activity requires functional FGF/mitogen-activated protein kinase signaling (Ribisi et al., 2000); however, this relationship is not reciprocal, as bFGF caudalizing activity per se is not dependent on XMeis3 activity. This result strongly supports a role for XMeis3 as a cell patterning protein that interprets and maintains a given AP status in the CNS.

The interpretation of experiments in which animal cap explants are caudalized by mouse Wnt3a is more complicated, but supportive of the results with bFGF. In *noggin/Wnt3a*-expressing caps, a similar rostralization was observed in the presence of XMeis3-AM, a gain of En2 expression, with a concomitant loss of *HoxB9*, *HoxB3* and *Krox20* expression. However, a somewhat contrasting result was seen with the co-injection of mouse *Wnt3a* and *XMeis3-AM* in the absence of noggin. In these experiments, there was indeed an increase in *En2* expression and a decrease in hindbrain marker expression, but we did not observe a reduction in *HoxB9* expression. In some experiments, we even saw an increase in *HoxB9* expression (not shown). It appears that in the absence of a strong neural inducer, mouse *Wnt3a* is a relatively weak inducer of hindbrain in comparison with *XMeis3*; however, mouse Wnt3a may actually induce spinal cord better than *XMeis3*. We have found that when *XMeis3* induces maximal levels of hindbrain markers, *HoxB9* expression is reduced in animal cap explants (not shown). Apparently, when mouse Wnt3a caudalizes alone, its induction of the *HoxB9* spinal cord marker is optimal when some *XMeis3* target genes are inhibited by the *XMeis3-AM*. Perhaps, antagonism of specific *XMeis3* target genes by the antimorph protein may enable mouse Wnt3a to more efficiently activate spinal cord markers instead of hindbrain markers in the absence of neural induction. However, in the presence of *noggin*, *XMeis3* target genes appear to be required for high *HoxB9* and hindbrain marker expression by mouse *Wnt3a*. In whole embryos, *HoxB9* expression is unchanged or even slightly increased in the presence of XMeis3-AM or the AMO. Inhibition of Xwnt-3a activity reduces *HoxB9* expression in embryos and explants (McGrew et al., 1997), so a delicate balance between Wnt and XMeis3 activities may maintain optimal *HoxB9* expression levels in the spinal cord. The implications of these wnt/XMeis3 interactions are still unclear, and further experiments are being carried out to understand how Wnt and XMeis3 pattern posterior neural tissue.

Using two distinct molecular approaches, we have inhibited XMeis3 protein activity in *Xenopus* embryos. In these embryos, a clear perturbation of the posterior CNS is observed, most specifically in the hindbrain region. XMeis3 appears to give distinct spatial identity to hindbrain cells. Without proper XMeis3 activity, anterior neural tissue spreads posteriorly and hindbrain identity is lost. The hindbrain is trapped in a more rostral cell fate. XMeis3 caudalizes the CNS to hindbrain, without inducing neural tissue. When viewing the 'activation' and 'transformation' model of neural induction, functional XMeis3 activity may be prerequisite for the 'transformation' step. XMeis3 probably interprets spatial information along AP axis in hindbrain cells, thus enabling them to differentiate in a proper manner. Future studies will focus on how XMeis3 functions as a transcriptional activator to caudalize the brain. By identifying genes directly targeted by XMeis3, we intend to determine the genetic hierarchy regulating hindbrain formation in the developing CNS.

REFERENCES

Baker J. C., Beddington R. S. and Harland R. M. (1999). Wnt signaling in Xenopus embryos inhibits bmp4 expression and activates neural development. *Genes Dev.* **23**, 3149-3159.

Blitz, I. L. and Cho, K, W. Y. (1995). Anterior neuroectoderm is progressively induced during gastrulation: the role of the *Xenopus* homeobox gene *orthodenticle*. *Development* **121**, 993-1004.

Bonstein, L., Elias, S. and Frank, D. (1998). Paraxial-fated mesoderm is required for neural crest induction in *Xenopus* embryos. *Dev. Biol.* **193**, 156-168.

Bradley, L., Snape, A., Bhatt, S. and Wilkinson, D. (1992). The structure and expression of the *Xenopus Krox-20* gene: Conserved and divergent patterns of expression in rhombomeres and neural crest. *Mech. Dev.* **40**, 73-84.

Cox, W. G and Hemmati-Brivanlou, A. (1995). Caudalization of neural fate by tissue recombination and bFGF. *Development* **121**, 4349-4358.

Doniach, T. (1993). Planar and vertical induction of anteroposterior patterning during the development of the Amphibia central nervous system. *J. Neurobiol.* **24**, 1256-1275.

Durston, A. Timmermans, J., Jage., W., Hendeiks, H., deVries, N., Heidveld, M. and Nieuwkoop, P. (1989). Retinoic acid causes an anteroposterior transformation in the developing central nervous system. *Nature* **340**, 140-144.

Fainsod, A., Deibler, K., Yelin, R., Marom, K., Epstein, M., Pillemer, G., Steinbeisser, H. and Blum, M. (1997). The dorsalizing and neural inducing gene follistatin is an antagonist of BMP-4. *Mech. Dev.* **63**, 39-50.

Gamse J. and Sive H. (2000). Vertebrate anteroposterior patterning: the Xenopus neurectoderm as a paradigm. *BioEssays* **11**, 976-986.

Godsave, S. F., Koster, C. H., Getahun, A., Mathu, M., Hooiveld, M., Van Der Wees, J., Hendriks, J. and Durston, A. J. (1998). Graded retinoid responses in the developing hindbrain. *Dev. Dyn.* **213**, 39-49.

Hamburger, V. (1988). *The Heritage of Experimental Embryology: Hans Spemann and the Organizer*. New York: Oxford University Press.

Harland, R. (1991). In situ hybridization: an improved whole mount method for *Xenopus* embryos. *Methods Cell Biol.* **36**, 685-695.

Harland, R. and Gerhart, J. (1997). Formation and function of Spemann's organizer. *Annu. Rev. Cell. Dev. Biol.* **13**, 611-667.

Heasman, J., Kofron, M. and Wylie, C. (2000). β-catenin signaling activity dissected in the early Xenopus embryo: a novel antisense approach. *Dev. Biol.* **222**, 124-134.

Hemmati-Brivanlou, A. and Harland, R. M. (1989). Expression of an *engrailed*-related protein in the anterior neural ectoderm of early *Xenopus* embryos. *Development* **106**, 611-617.

Hemmati-Brivanlou, A., Frank, D., Bolce, M. E., Brown, B. D., Sive, H. L. and Harland, R. M. (1990). Localization of specific mRNAs in *Xenopus* embryos by whole-mount in situ hybridization. *Development* **110**, 325-330.

Hemmati-Brivanlou, A. and Melton, D. A. (1994). Inhibition of activin receptor signaling promotes neuralization in *Xenopus*. *Cell* **77**, 273-281.

Henig, C., Elias, S. and Frank, D. (1998). A POU protein regulates mesodermal competence to FGF in Xenopus. *Mech. Dev.* **71**, 131-142.

Hollemann, T., Chen, Y., Grunz, H. and Pieler, T. (1998). Regionalized metabolic activity establishes bouundaries of retinoic acid signalling. *EMBO J.* **17**, 7361-7372.

Hooiveld, M. H., Morgan R., in der Rieden P., Houtzager E., Pannese M., Damen K., Boncinelli E. and Durston, A. J. (1999). Novel interactions between vertebrate *Hox* genes. *Int. J. Dev. Biol.* **43**, 665-674.

Hsu, D. R., Economides, A. N., Wang, X., Eimon, P. M. and Harland, R. M. (1998). The *Xenopus* dorsalizing factor Gremlin identifies a novel family of secreted proteins that antagonize BMP activities. *Mol. Cell* **5**, 673-683.

Inbal, A., Halachmi, N., Dibner, C., Frank, D. and Salzberg, A. (2001). Genetic evidence for the transcriptional-activating function of Homothorax during adult fly development. *Development* **128**, 3405-3413.

Kao, K. R. and Elinson, R. P. (1988). The entire mesodermal mantle behaves as Spemann's organizer in dorsoanterior enhanced *Xenopus laevis* embryos. *Dev. Biol.* **127**, 64-77.

Kenkgaku, M. and Okamoto, H. (1995). bFGF as a possible morphogen for the anteroposterior axis of the central nervous system in *Xenopus*. *Development* **121**, 3121-3130.

Kessler, D. (1995). Siamois is required for the formation of Spemann's organizer *Proc. Natl. Acad. Sci. USA* **94**, 13017-13022.

Knecht, A. K., Good, P. J., Dawid, I. B. and Harland, R. M. (1995). Dorsal-ventral patterning and differentiation of noggin induced neural tissue in the absence of mesoderm. *Development* **121**, 1927-1936.

Kolm, P. J. and Sive, H. (1995). Hindbrain patterning requires retinoid signaling. *Dev. Biol.* **192**, 1-16.

Kolm, P. J., Apekin, V. and Sive, H. (1997). Regulation of *Xenopus* labial homeodomain genes, *HoxA1* and *HoxD1*: Activation by retinoids and peptide growth factors. *Dev. Biol.* **167**, 34-49.

Kurant, E., Pai, C. Y., Sharf, R., Halachmi, N., Sun, Y. H. and Salzberg, A. (1998). *dorsotonals/homothorax*, the *Drosophila* homologue of *meis-1*, interacts with *extradenticle* in patterning of the embryonic PNS. *Development* **125**, 1037-1048.

Lamb, T. M., Knecht,. A. K., Smith, W. C., Stachel, S. E., Economides, A., Stahl, N., Yancopolous, G. D. and Harland, R. M. (1994). Neural induction by a secreted polypeptide noggin. *Science* **262**, 713-718.

Lamb, T. M. and Harland, R. M. (1995). Fibroblast growth factor is a direct neural inducer, which combined with noggin generates anterior-posterior neural pattern. *Development* **121**, 3627-3636.

Maeda, R., Mood, K., Jones, T. L., Aruga, J., Buchberg, A. M. and Daar, I. O. (2001). *Xmeis1*, a protooncogene involved in specifying neural crest cell fate in *Xenopus* embryos. *Oncogene* **20**, 1329-1342.

McGrew, L. L., Lai, C. J. and Moon, R. T. (1995). Specification of the anteroposterior neural axis through synergistic intraction of the Wnt signaling cascade with noggin and follistatin. *Dev. Biol.* **172**, 337-342.

McGrew, L. L., Hoppler, S. and Moon, R. T. (1997). Wnt and FGF pathways cooperatively pattern anteroposterior neural ectoderm in *Xenopus*. *Mech. Dev.* **69**, 105-114.

Nasevicius, A. and Ekker, S. C. (2000). Effective targeted gene 'knockdown' in zebrafish. *Nat. Genet.* **2**, 16-20.

Nieuwkoop, P. (1952). Activation and organization of the central nervous system in amphibians III. Synthesis of a new working hypothesis. *J. Exp. Zool.* **120**, 83-108.

Nieuwkoop, P. and Faber, J. (1967). *Normal Table of* Xenopus laevis *(Daudin)*. Amsterdam: North-Holland Publishing Company.

Papalopulu, N. and Kintner, C. (1996). A posteriorizing factor, retinoic acid, reveals that anteroposterior patterning controls timing of neuronal differentiation in *Xenopus* neuroectoderm. *Development* **122**, 3409-3418.

Piccolo, S., Sasai, Y., Lu, B. and De Robertis, E. (1996). Dorsoventral patterning in *Xenopus*: Inhibition of ventral signals by direct binding of chordin to BMP-4. *Cell* **86**, 589-598.

Re'em-Kalma, Y., Lamb, T. and Frank, D. (1995). Competition between noggin and bone morphogenetic protein 4 activities may regulate dorsalization during *Xenopus* development. *Proc. Natl. Acad. Sci. USA* **92**, 12141-12145.

Ribisi S. Jr., Mariani F. V., Aamar E., Lamb T. M., Frank D. and Harland R. M. (2000). Ras-mediated FGF signaling is required for the formation of posterior but not anterior neural tissue in Xenopus laevis. *Dev. Biol.* **227**, 183-196.

Richter, K. H., Grunz, H. and Dawid, I. B. (1988). Gene expression in the embryonic nervous system of *Xenopus laevis*. *Proc. Natl. Acad. Sci. USA* **85**, 8086-8090.

Rieckhof, G. E., Casares, F., Ryoo, H. D., Abu-Shaar, M. and Mann, R. (1997). Nuclear translocation of extradenticle requires *homothorax*, which encodes an extradenticle-related homeodomain protein. *Cell* **91**, 171-183.

Ruiz i Altaba, A. and Jessell, T. (1991). Retinoic acid modifies the pattern of cell differentiation in the central nervous system of neurula stage *Xenopus* embryos. *Development* **112**, 945-958.

Salzberg, A., Elias, S., Nachaliel, N., Bonstein, L., Henig, C. and Frank, D. (1999). A Meis family protein caudalizes neural cell fates in *Xenopus*. *Mech. Dev.* **80**, 3-13.

Sasai, Y., Lu, B., Steinbeisser, H., Geissert, D., Gont, L. K. and DeRobertis, E. (1994). *Xenopus* chordin: a novel dorsalizing factor activated by organizer-specific homeobox genes. *Cell* **79**, 779-790.

Sharpe, C. (1991). Retinoic acid can mimic endogenous signals involved in transformation of the *Xenopus* nervous system. *Neuron* **7**, 239-247.

Sive, H. L., Hattori, K. and Weintraub, H. (1989). Progressive determination during formation of the anteroposterior axis in *Xenopus laevis*. *Cell* **58**, 171-180.

Sive, H, Draper, B., Harland, R. and Weintraub, H. (1990). Identification of a retinoic acid sensitive period during primary axis formation in *Xenopus laevis*. *Genes Dev.* **4**, 932-942.

Smith, W. C. and Harland, R. M. (1991). Injected Xwnt-8 RNA acts early in *Xenopus* embryos to promote formation of a vegetal dorsalizing center. *Cell* **67**, 753-765.

Smith W. C. and Harland R. M. (1992). Expression cloning of noggin, a new dorsalizing factor localized to the Spemann organizer in Xenopus embryos. *Cell* **70**, 829-840.

Weinstein, D. C., Rahman, S. M., Ruiz, J. C. and Hemmati-Brivanlou, A. (1996). Embryonic expression of *eph* signaling factors in *Xenopus*. *Mech. Dev.* **57**, 133-144.

Wilson, P. A. and Melton, D. A. (1994). Mesodermal patterning by an inducer gradient depends on secondary cell-cell communication. *Curr. Biol.* **4**, 676-686.

Wright, C. V. E., Morita, E. A., Wilkin, D. J. and de Robertis, E. M. (1990). The *Xenopus* XlHbox6 homeo protein, a marker of posterior neural induction, is expressed in proliferating neurons. *Development* **109**, 225-234.

Zimmerman, L. B., De Jesus-Escobar, J. M. and Harland, R. M. (1996). The Spemann organizer signal noggin binds and inactivates bone morphogenetic protein 4. *Cell* **86**, 599-606.